A novel antifuse structure based on amorphous bismuth zinc niobate thin films*

Wang Gang(王刚)†, Li Wei(李威), Li Ping(李平), Li Zuxiong(李祖雄), Fan Xue(范雪), and Jiang Jing(姜晶)

State Key Laboratory of Electronic Thin Films and Integrated Devices, University of Electronic Science and Technology of China, Chengdu 610054, China

Abstract: A novel antifuse structure with amorphous bismuth zinc niobate (a-BZN) dielectrics was proposed. The characteristics of the a-BZN antifuse were investigated. Programming direction of up to down was chosen to rupture the a-BZN antifuse. The breakdown voltage of the a-BZN antifuse was obtained at a magnitude of 6.56 V. A large off-state resistance of more than 1 GΩ for the a-BZN antifuse was demonstrated. The surface micrograph of the ruptured a-BZN antifuses was illustrated. Programming characteristics with the programming time of 0.46 ms and on-state properties with the average resistance value of 26.1 Ω of the a-BZN antifuse were exhibited. The difference of characteristics of the a-BZN antifuse from that of a cubic pyrochlore bismuth zinc niobate (cp-BZN) antifuse and gate oxide antifuse was compared and analyzed.

Key words: amorphous bismuth zinc niobate; thin film; antifuse; comparison
DOI: 10.1088/1674-4926/33/8/084002 **EEACC:** 2520; 2560

1. Introduction

The antifuse, as a one time programmable switch element, has been applied in a large number of fields such as programmable read only memory (PROM) and field programmable gate arrays (FPGAs)[1−3]. Typical antifuse structures are oxide–nitride–oxide (ONO) and amorphous silicon (a-Si) antifuses. However, the ONO and a-Si antifuses are not compatible with the standard CMOS technology[4, 5]. Recently, the gate oxide antifuse has been paid more and more attention due to its compatibility with standard CMOS technology[6−9]. But, with quick progress of the CMOS technology, the thickness of the gate insulator has reduced to about 1 nm, resulting in some reliability issues[10] of the device based on gate dielectric. Now, it is important to find an alternative high-k material to replace SiO_2 as the gate insulator for gate dielectric devices.

In our previous report, the cubic pyrochlore bismuth zinc niobate (cp-BZN) thin film as an alternative high-k material had been proposed to form an antifuse structure, and the excellent characteristics of the cp-BZN antifuse had been investigated[11]. However, the deposition temperature for the cp-BZN materials is high, up to 750 ℃ which increases the thermal budget and restricts the application of the antifuse with low melting point metal electrodes，such as aluminum. Consequently, lowering the manufacturing temperature of the BZN thin film is desirable. It is reported that the BZN thin film prepared at room temperature exhibits a high permittivity larger than 51, and the leakage current of the thin film is approximately 10^{-7} A/cm^2 at an applied bias of 5 V[12]. The dielectric constant of the BZN thin film fabricated by the sol-gel technique is about 91[13]. The BZN thin films deposited at a low temperature exhibit an amorphous phase. To date, the amorphous BZN (a-BZN) thin film has been integrated with transistors and printed circuit boards[14−16]. However, little is known about the characteristics of the antifuse based on a-BZN thin films. This is an interesting area of research.

In this study, the properties of a novel antifuse with a-BZN thin films were investigated. A metal to metal structure for the a-BZN antifuse similar to a cp-BZN antifuse was used. The off-state properties of the a-BZN antifuse were demonstrated in terms of breakdown voltage, programming direction, and leakage currents. After breakdown, the surface micrograph of the antifuses was illustrated. The a-BZN antifuses were programmed with a higher voltage compared to the breakdown voltage, and the programming time and current were obtained. Ultimately, the resistance distribution for the programmed antifuses was presented. The difference of properties between a-BZN and cp-BZN antifuse was compared and analyzed.

2. Experiments

The schematic cross section for the a-BZN antifuses is shown in Fig. 1. A silicon substrate with 0.6 μm thick thermal SiO_2 was used. The Pt thin film, as the bottom electrode of the a-BZN antifuses, was deposited using RF magnetron sputtering methods with a thickness of 150 nm, where a 50 nm Ti thin film was used as an adhesion layer. The amorphous $Bi_{1.5}Zn_{1.0}Nb_{1.5}O_7$ (a-BZN) thin film was prepared at 300 ℃ by RF magnetron sputtering, where the sputtering gas mixtures were Ar and O_2 at a flow rate of 42.5 sccm and 7.5 sccm, respectively. The thickness of the a-BZN thin films deposited for 1 h was approximately 100 nm. The XRD patterns of the BZN thin films deposited at 750 and 300 ℃ are shown in Fig. 2. At 300 ℃ the phase of the BZN thin film was amorphous. For electrical measurements, 200 nm thick Al thin films as top electrodes were deposited through shadow masks with a diameter of 200 μm.

* Project supported by the Opening Project of State Key Laboratory of Electronic Thin Films and Integrated Devices (No. KFJJ200909).
† Corresponding author. Email: wgphd@163.com
Received 10 February 2012, revised manuscript received 11 April 2012

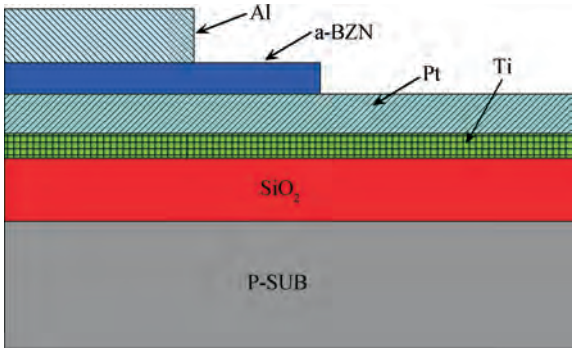

Fig. 1. Schematic cross section of the amorphous BZN antifuse.

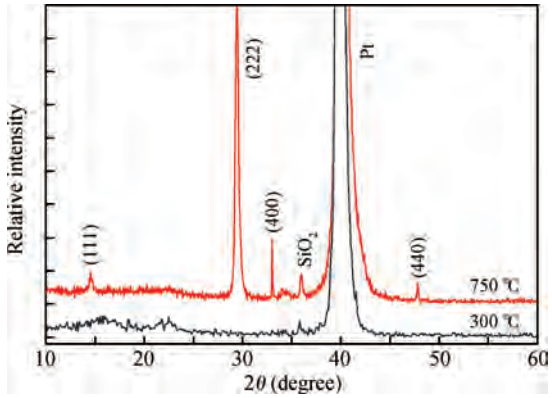

Fig. 2. XRD patterns of the BZN thin films deposited at 750 and 300 ℃.

A Cascade probe station was used to fix and test the a-BZN antifuse samples. The Agilent 4155B semiconductor parameter analyzer was selected to perform the characteristics of the antifuses. During experiments, programming directions were varied by changing the positive bias connected to the top or bottom electrodes. The surface micrograph of the ruptured a-BZN antifuses was illustrated through an optical microscope. To limit the discharge current of the capacitors during programming, some series resistors connected to the probe were used.

3. Results and discussion

To rupture and program the a-BZN antifuses, two programming directions should be used: the top electrode was applied with positive bias and the bottom electrode with ground potential as up to down direction; the bottom electrode connected to positive potential and the top electrode grounded as down to up directions. The off state characteristics of the a-BZN antifuses with different programming directions mentioned above are shown in Fig. 3. It was shown that the breakdown voltage was approximately 6.56 V for up to down directions and about 12.48 V for down to up directions. In the case of the leakage current, there was only a little difference between the up to down direction and down to up directions when the applied voltage was less than 6.56 V. The value of the leakage current for the up to down direction was nearly 2×10^{-6} A associated with the breakdown voltage of 6.56 V, and for down to up directions the value was approximately 6×10^{-4} A associated

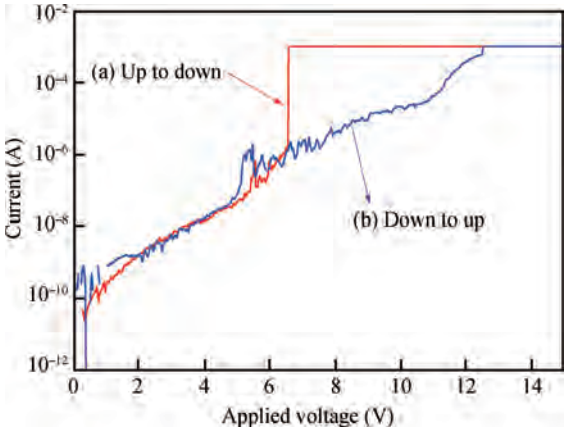

Fig. 3. Off state characteristics of the a-BZN antifuses with the programming direction (a) up to down and (b) down to up.

with the breakdown voltage of 12.48 V. Influences of the different leakage currents and breakdown voltages on the top electrodes of the ruptured a-BZN antifuses will be discussed later. Furthermore, the leakage current was approximately 10^{-9} A for both up to down and down to up programming directions at the applied bias of 2 V indicating that the off state resistance of the a-BZN antifuses was larger than 1 GΩ, which was better for decreasing the static power dissipation of the devices based on the antifuses.

With the increase of the scanning voltage applied to the electrode of the antifuse, some traps in the dielectrics were collected, and then, a path for leakage current was formed. Lastly, the dielectric was ruptured. The cp-BZN thin film was composed of crystal grains of a large size; however, the a-BZN thin film was composed of a great number of fine particles. The leakage current path was formed more easily in the cp-BZN antifuse than that in the a-BZN antifuse due to the fact that the cp-BZN thin film was not compact. As a result, the leakage current flowing through the a-BZN antifuse was small; in the other hand, the breakdown voltage for the a-BZN antifuse was larger than that for the cp-BZN antifuse. At 4 V, the value of the leakage current of the a-BZN antifuse with up to down and down to up programming directions was about 1 order and 3 orders less than that of cp-BZN antifuse, respectively. In the case of the breakdown voltage, the magnitude for the a-BZN antifuse with up to down and down to up programming directions was increased by approximately 1.96 V and 0.48 V compared to the cp-BZN antifuse, respectively.

In Fig. 3, it was shown that the breakdown characteristics and leakage current characteristics of the a-BZN antifuses were varied due to different programming directions. In addition, the influence of various programming directions on the top electrodes of the ruptured a-BZN antifuses was different which was illustrated in Fig. 4. For up to down programming directions, the surface of the top electrodes of the programmed a-BZN antifuses was smooth and clean. In contrast, the surface was filled with black spots for down to up programming directions.

The structure of the a-BZN antifuses was SiO_2/Ti/Pt/a-BZN/Al. For up to down programming directions, the electrons forming a leakage current were injected from the bottom electrode, Pt thin film, into the a-BZN insulators; in the con-

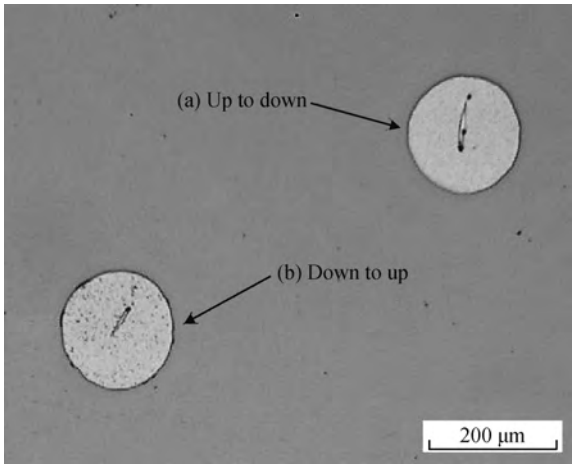

Fig. 4. Surface micrographs of the top electrode of the ruptured a-BZN antifuses with programming directions (a) up to down and (b) down to up.

trary direction, the electrons were injected from the Al electrodes. With up to down programming directions, the Pt electrode would be melted during programming, and then diffused into the a-BZN insulators in the electron flowing direction. In the other direction, the molten Al electrode would diffuse into the a-BZN insulators. Finally, a conductive filament was formed between the top and bottom electrode, and the antifuse was programmed successfully. The interface states between the Pt/a-BZN and the Al/a-BZN were different, and also the properties between the Pt and the Al electrode were varied, which resulted in different breakdown voltages for various programming directions shown in Fig. 3. When the applied voltage was less than 6.56 V, associated with the breakdown voltage of up to down programming directions, the leakage currents flowing through the antifuses with both programming directions were almost the same. However, more leakage current and more bias had to be applied to the antifuse with the down to up programming direction to make the antifuses rupture compared to the up to down programming directions. Lots of thermal energy caused by Joule heat should be diffused through the down to up programming antifuses before the antifuse ruptures. We think the thermal energy caused the oxidization of the aluminum top electrode with the oxygen in the air, and then some black spots emerged as shown in Fig. 4(b).

The programming characteristic of the a-BZN antifuses is shown in Fig. 5. A programming voltage of 7.5 V, which was about 14.3 % larger than the breakdown voltage, was used to rupture and program the a-BZN antifuse, where the programming direction was up to down. To limit the current flowing through the programmed antifuses, a compliance current of 1 mA was set. The currents flowing through the a-BZN antifuse as a function of programming time for some typical antifuse samples are shown in Fig. 5(a). Figure 5(b) shows the distribution of programming times for the programmed a-BZN antifuses. The programming times exhibited a tight distribution with the average magnitude of approximately 0.46 ms, where the standard deviation was about 0.20 ms. Compared to the cp-BZN antifuse, the programming voltage of the a-BZN antifuse was increased by about 36.4 %; however, the average programming time was reduced in a magnitude of 77 %, while the programming current showed almost no change. In addition, the a-BZN antifuses showed a better programming characteristic than that of gate oxide antifuses[6−8].

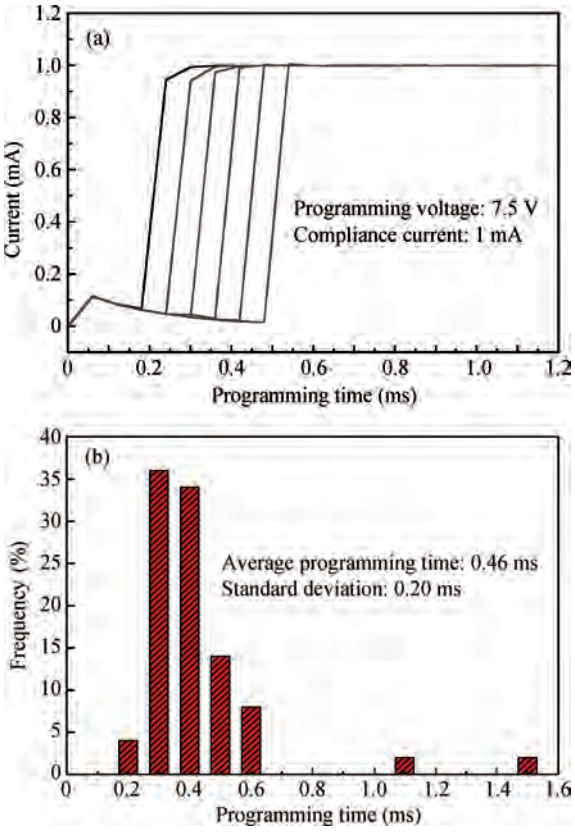

Fig. 5. Programming characteristics of the a-BZN antifuses. (a) Current flowing through the a-BZN antifuse as a function of programming time. (b) Distribution of programming times for programmed a-BZN antifuses.

Figure 6 demonstrates the resistance distribution and cumulative distribution of the on state resistance of the programmed a-BZN antifuses. A tight distribution of the programmed antifuse resistances for the a-BZN antifuse is shown in Fig. 6(a). The cumulative distribution of the programmed antifuse resistance of the a-BZN antifuses is illustrated in Fig. 6(b), where the inset was the cumulative distribution of the programmed antifuse resistance for gate oxide antifuse fabricated with the TSMC 0.18 μm CMOS process. In Fig. 6(b), it was illustrated that the distribution range of the programmed antifuse resistance for the programmed a-BZN antifuse was within several hundred ohms; however, the distribution range for the gate oxide antifuse was larger than several thousand ohms which was in agreement with the reported results[6]. The average on state resistance for the programmed a-BZN antifuses was approximately 26.1 Ω, which was sufficiently lower than that for gate oxide antifuse[6−8]. Compared to cp-BZN antifuse, the on state resistance of the a-BZN antifuse was increased by about 8.6 Ω. The energy applied for programming the cp-BZN antifuse was about 11.66 μJ, and the value was approximately 3.45 μJ for a-BZN antifuse. Less energy was used for programming the a-BZN antifuse than the cp-BZN antifuse, which resulted in a higher on state resistance of the a-BZN antifuse.

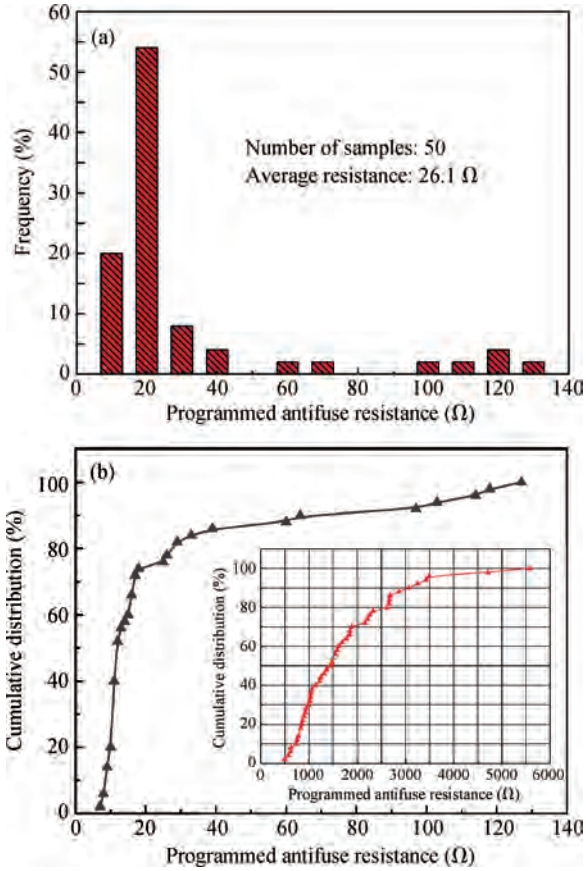

Fig. 6. On state properties of the a-BZN antifuse. (a) Resistance distribution of the on state resistance of the programmed a-BZN antifuses. (b) Cumulative distribution of the on state resistance of the programmed a-BZN antifuses. The inset was cumulative distribution of the programmed antifuse resistance for gate oxide antifuse fabricated with the TSMC 0.18 μm CMOS process.

4. Conclusion

In this research, we have investigated the characteristics of a novel antifuse with the structure of Ti/Pt/a-BZN/Al. The difference of the interface states between Pt/a-BZN and Al/a-BZN, and the difference of properties between Pt and Al electrodes caused different breakdown voltages of the a-BZN antifuses applied with various programming directions. For down to up programming directions, more leakage current and more bias should be added to the antifuses to rupture the a-BZN dielectrics compared to the up to down programming directions, resulting in lots of thermal energy diffused through the antifuses and the oxidization of the Al top electrodes. Therefore, the programming direction of up to down was proposed to program and rupture the a-BZN antifuses. The a-BZN antifuses presented an excellent off state property with the off state resistance larger than 1 GΩ. Compared to the cp-BZN antifuse, the a-BZN antifuse exhibited higher breakdown voltages and on state resistances; however, the leakage current, programming time, and programming energy of the a-BZN antifuse were less. In addition, compared to the gate oxide antifuses, the a-BZN antifuse not only showed good programming characteristics but also exhibited a better on state property. However, to further improve the properties of a-BZN antifuses, a great amount of work should be done including improving the quality of the a-BZN insulators and improving the interface qualities between the electrodes and insulators.

Acknowledgments

The authors would like to thank Dr. Li Ruguan for preparing the a-BZN thin films and for valuable discussions. We also acknowledge Dr. Chu Futong for XRD measurements.

References

[1] Greene J, Hamdy E, Beal S. Antifuse field programmable gate arrays. Proc IEEE, 1993, 81(7): 1042
[2] Hamdy E, McCollum J, Chen S, et al. Dielectric based antifuse for logic and memory ICs. IEDM Tech Dig, 1988: 786
[3] McCollum J. ASIC versus antifuse FPGA reliability. Aero Conf IEEE, 2009: 1
[4] Chen J, Eltoukhy S, Yen S, et al. A modular 0.8 μm technology for high performance dielectric antifuse field programmable gate arrays. Proc VTSA, 1993: 160
[5] Vasudevan N, Fair R B, Massoud H Z, et al. On-state reliability of amorphous-silicon antifuse. J Appl Phys, 1998, 84(11): 6440
[6] Kim J, Lee K. Three-transistor one-time programmable (OTP) ROM cell array using standard CMOS gate oxide antifuse. IEEE Electron Device Lett, 2003, 24(9): 589
[7] Cha H-K, Yun I, Kim J, et al. A 32-kB standard CMOS antifuse one-time programmable ROM embedded in a 16-bit microcontroller. IEEE J Solid-State Circuits, 2006, 41(9): 2115
[8] Kim J, Lee K. 3-transistor cell OTP ROM array using standard CMOS gate-oxide antifuses. J Semicond Technol Sci, 2003, 3(4): 205
[9] Deloge M, Allard B, Candelier P, et al. Application of a TDDB model to the optimization of the programming voltage and dimensions of antifuse bitcells. IEEE Electron Device Lett, 2011, 32(8): 1041
[10] Wilk G D, Wallace R M, Anthony J M. High-k gate dielectrics: current status and materials properties considerations. J Appl Phys, 2001, 89(10): 5243
[11] Wang G, Li W, Li P, et al. Cubic pyrochlore bismuth zinc niobate thin films for antifuse applications. IEEE Electron Device Lett, 2012, 33(1): 92
[12] Kim I D, Lim M H, Kang K T, et al. Room temperature fabricated ZnO thin film transistor using high-k $Bi_{1.5}Zn_{1.0}Nb_{1.5}O_7$ gate insulator prepared by sputtering. Appl Phys Lett, 2006, 89(2): 022905
[13] Shu B, Zhang H M, W Q, et al. Bi_2O_3–ZnO–Nb_2O_5 film fabricated by sol–gel technique and C–V characteristic of GaN MIS structure. J Semicond, 2007, 28(9): 1406
[14] Lim M H, Kang K T, Kim H G, et al. Low leakage current stacked MgO/$Bi_{1.5}Zn_{1.0}Nb_{1.5}O_7$ gate insulator for low voltage ZnO thin film transistors. Appl Phys Lett, 2006, 89(20): 202908
[15] Choi Y, Kim I D, Tuller H L, et al. Low-voltage organic transistors and depletion-load inverters with high-k pyrochlore BZN gate dielectric on polymer substrate. IEEE Trans Electron Devices, 2005, 52(12): 2819
[16] Park J H, Lee W S, Seong N J, et al. Bismuth-zinc-niobate embedded capacitors grown at room temperature for printed circuit board applications. Appl Phys Lett, 2006, 88(19): 192902